Landslides (2017) 14:1225–1233
DOI 10.1007/s10346-016-0779-2
Received: 2 December 2015
Accepted: 13 November 2016
Published online: 19 November 2016

Paulina Harba · Zenon Pilecki

Assessment of time–spatial changes of shear wave velocities of flysch formation prone to mass movements by seismic interferometry with the use of ambient noise

Abstract This paper presents the results of monitoring flysch formation shear wave velocities at varying conditions of water content by seismic interferometry. Studies were conducted on a section of the active Just-Tegoborze landslide in the southern region of Poland. The landslide is intersected by the state road no. 75, which has a high traffic density. Measurements of the seismic interferometry were made on the basis of the registration of a local high-frequency noise generated mostly by passing heavy vehicles. Measurements were carried out in three series on January, March and July in 2015. Seismic noise vibration was registered using Güralp CMG-6TD broadband seismometers. One of the seismic profiles was located along a geological engineering cross-section prepared from research boreholes data. One of the main results of the work was the sections of changes of shear wave velocity. The interpreted seismic boundaries made it possible to correlate them with the lithological ones. The trough-like shape of the bedrock boundary may be an effect of weathering processes developed in the zone consisting of weak hieroglyphic beds. It is also supposed to be one of the slip surfaces. The seismic sections of shear wave velocity allowed to analyse velocity variations between three measurement series and to compare them with expected water content in colluvium deposits. The presented results of the study confirmed the utility of seismic interferometry based on ambient noise registration in evaluating the behaviour of landslides in the Carpathian flysch formation.

Keywords Landslide · Seismic interferometry · Ambient noise · Carpathian flysch

Introduction

The recognition of landslide behaviour in various geological conditions is crucial in landslide hazard evaluation (Aleotti and Chowdhury 1999; Anbarasu et al. 2010; Guzzetti et al. 1999; Dai et al. 2002; Barla et al. 2013; Bonnard and Corominas 2005; Cascini et al. 2005; Fukuoka et al. 2005; Mansour et al. 2011; Sassa et al. 2004, Song and Kim 2014). In this sense, geophysical methods may be helpful in monitoring landslides and, consequently, in assessing the landslide hazard (Bichler et al. 2004; Bièvre et al. 2015; Brückl et al. 2013; Bogoslovsky and Ogilvy 1977; Frasheri et al. 1998; Hack 2000; Méric et al. 2005; Jongmans and Garambois 2007; Jongmans et al. 2009; Lundström et al. 2009; Hibert et al. 2011; Reynolds 2011, Salas-Romero et al. 2015; Singh et al. 2013; Travelletti et al. 2013; Zarroca et al. 2014). In recent years, a new seismic method based on ambient noise has been intensively developed, known as seismic interferometry, which may be demonstrated to be useful in monitoring mass movements (Jongmans and Garambois 2007; Méric et al. 2007; Jongmans et al. 2009; Renalier et al. 2010a, 2010b; Mainsant et al. 2012b; Del Gaudio et al. 2013; Pilz et al. 2013).

Seismic interferometry is a method enabling the use of local seismic noise for analysis of changes of elastic properties within the geological medium. It is originated from the phenomenon of interference of seismic signals (Curtis et al. 2006; Schuster 2009). The principles and applications of seismic interferometry were broadly explained by Schuster (2009) and Wapenaar et al. (2010a, 2010b).

Seismic interferometry consists of retrieving the impulse response of the medium, the so-called Green's function, between a pair of receivers using the operations of cross-correlation, deconvolution or cross-coherence of seismic signals registered at the receivers. The method assumes a Rayleigh surface wave, which is dispersive, i.e., its velocity strictly depends on the frequency. Rayleigh waves are described by dispersion curves, which demonstrate the dependence of a phase velocity on wave frequency. Shear wave (S-wave) velocities have the dominant influence on the dispersion curve in a high-frequency range (>5 Hz) (Xia et al. 1999). As a result of inversion of a Rayleigh wave's phase velocity, an image of the changes in S-wave velocities is obtained. The S-wave velocity is sensitive to changes in properties of the ground medium, especially to changes in its rigidity, which could be also the consequence of changes in water content in the medium.

Seismic interferometry has increasing geo-engineering applications. Larose et al. (2015) presented recent developments in ambient seismic noise methods to monitor the variations in the mechanical properties of the subsurface and to identify new sources of seismic signals that occur outside the solid Earth. The authors demonstrated the use of seismic noise in marking the thermal variations in the subsoil, in buildings or in rock columns, the temporal and spatial evolution of a water table and the changes of the rigidity of the soil constituting a slope prone to mass movements.

Seismic interferometry studies analysing changes in the S-wave velocity preceding major landslide movements were broadly undertaken by Mainsant et al. (2012b). These researchers concluded that the observed changes in the S-wave velocity decreased two or even threefold before mass movement. The drop in S-wave velocities was correlated with the measurements of displacement performed on the terrain surface. Moreover, Mainsant et al. (2012a) studied the S-wave velocity in terms of rheological changes in clay-rich geological formations, which are responsible for many landslides. These researchers conducted rheometrical laboratory experiments to investigate the solid-fluid transition, which affects derangement of the particle network and is associated with a loss in rigidity. The results indicated that the S-wave velocity significantly varies with rheological changes in the clay, supposedly caused by the disorganization of the particle network. According to the outcomes of their investigations, the authors concluded that measuring the S-wave velocity could be applicable to monitoring

rheological changes in landslides in clayey deposits and that the time-dependent variation in this parameter could be a beneficial indicator for earthflows. The authors continued laboratory experiments (Mainsant et al. 2015) in order to examine the physical origin of the S-wave velocity decreases which occur prior to the onset of mass movements. Additional rheometrical studies indicated that it is probably caused by a complex transient rheological response of the clay. These researchers supposed that such response is connected to the existence of the so-called "delayed fluidization" phases in which the shear modulus quickly decreases while the apparent viscosity varies more slowly and requires more time to reach its fluid level. The results are comparable with a real in-field situation of a landslide movement.

Renalier et al. (2010a) applied ambient seismic measurements to determine the deepest slip surface of a landslide in clayey deposits, which had not been detected by active seismic methods. This surface was found by obtaining the dispersion curves at lower frequencies than 3 Hz. During a 30-month period of seismic noise observations, they detected a slight but significant decrease in the surface wave velocities. Moreover, authors observed both lateral and vertical variations of the S-wave velocity which have been related to landslide activity and the location of slip surfaces. Additionally, Renalier et al. (2010b) successfully applied an ambient noise cross-correlation to obtain a 3D model of the S-wave velocity of a landslide affecting clayey deposits. They computed cross-correlations between the vertical components of recording stations which allowed them to retrieve the Rayleigh wave Green's functions and estimate their group velocity dispersion curves in the 1.7–5 Hz frequency range. The dispersion curves were then inverted with a neighbourhood algorithm which resulted in the 3D model of the S-wave velocity of the studied landslide.

The results of seismic studies described in this paper are a continuation of the work by Pilecki and Harba (2015) who presented the usefulness of the seismic interferometry method in mapping the structure and properties of the near-surface geological medium in the area of the active Just-Tegoborze landslide (southern Poland). Their preliminary results are based on the measurements carried out along single seismic profile in two measurement series. In this paper, we present the results developed with one additional series. Moreover, the results were extended with data from transverse seismic profiles. We also describe the geological conditions of the Just-Tegoborze landslide and the measurement methodology, as well as the methodology of seismic data processing and interpretation. The changes of elastic properties of geological medium are characterized by the changes in the S-wave velocity. The recognized seismic boundaries are correlated to lithological ones shown on the geological engineering cross-section.

Geological and geomorphological setting

Geographically, the Just-Tegoborze landslide is located in Swidnik and Tegoborze villages, in Nowy Sacz county in the southern part of Poland. It is situated on a slope of Jodlowiec Wielki Mountain and St. Just Mountain, slightly below St. Just pass of the Beskid Wyspowy range (Fig. 1).

From the geological point of view, the Just-Tegoborze landslide lies in Magura Nappe in the Outer (Flysch) Carpathians (Fig. 2). On the study area, Magura Nappe is represented by hieroglyphic beds, Magura beds and Sub-Magura beds. Hieroglyphic beds are mainly built of thin-bedded sandstones and shales. They are interbedded with medium and thick-bedded sandstones in the upper part, whereas shales constitute a majority in the lower part. Magura beds consist of muscovitic sandstones of 0.7 to 2 m thickness. Sub-Magura beds are built of sandstones and shales. Flysch formation, according to data from the 3I/P borehole located on the study area (Fig. 3), dips at angles from 60° to 84° toward the North.

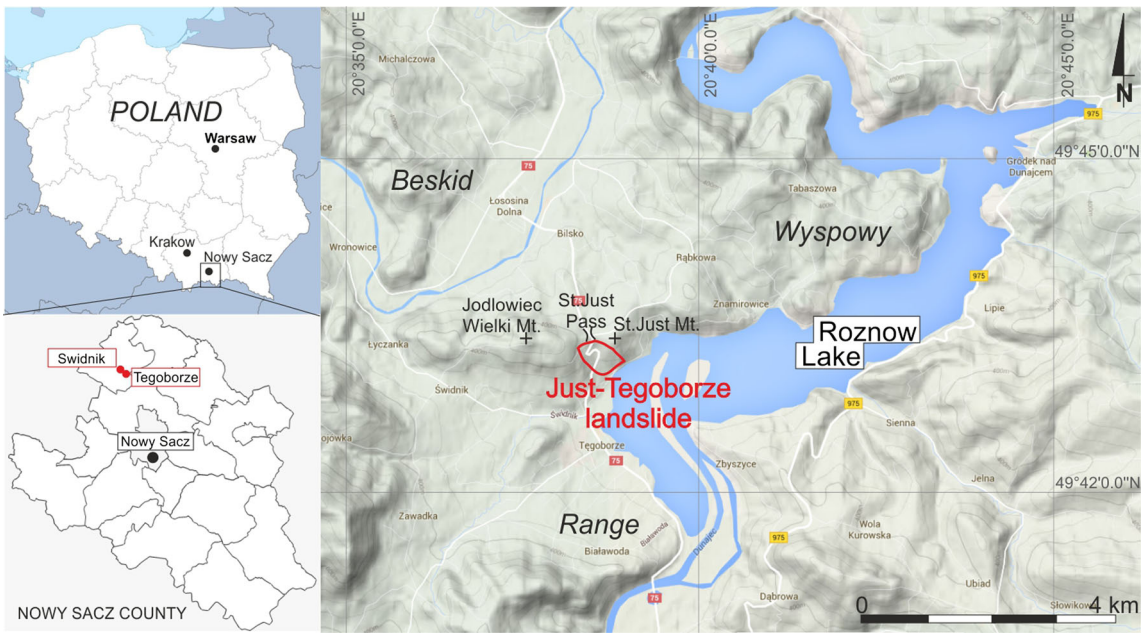

Fig. 1 Geographic location map of the study area of the Just-Tegoborze landslide (on the basis of Google Maps)

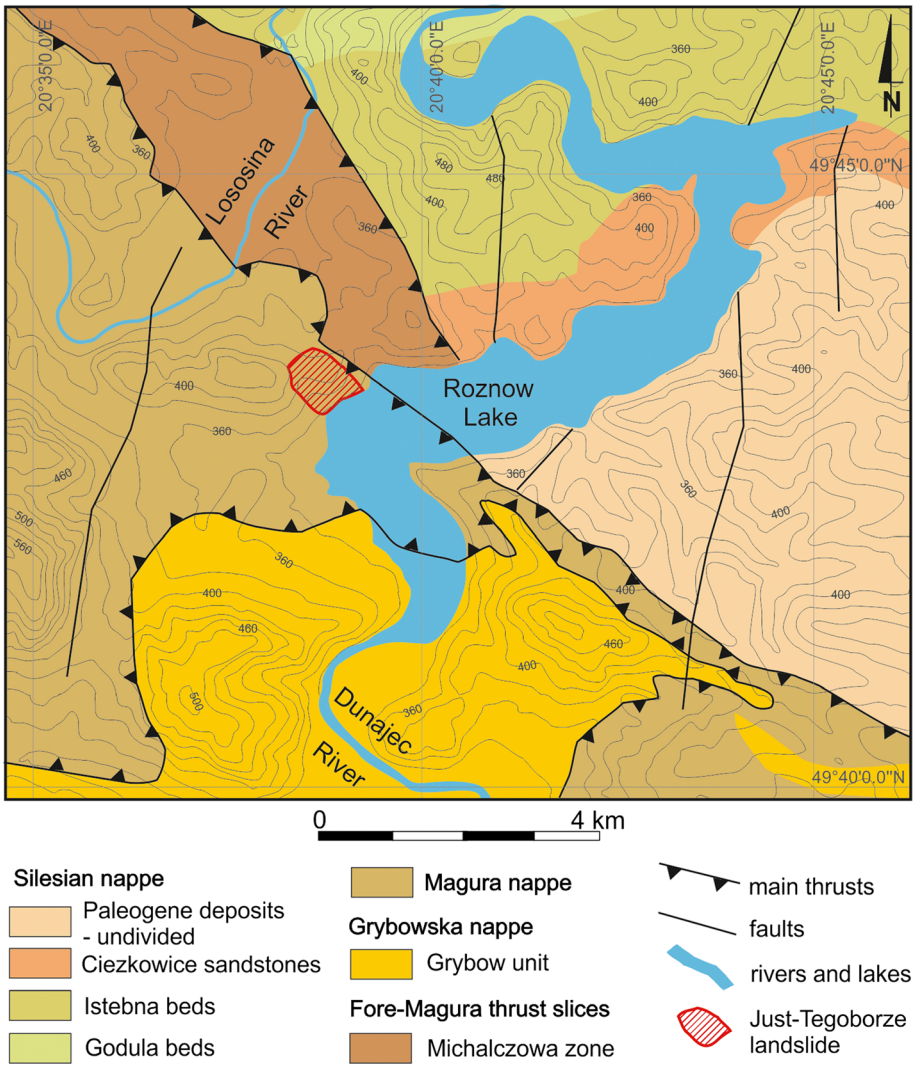

Fig. 2 Geological map of the surrounding area of the Just-Tegoborze landslide with elevation contour lines marked (based on Cieszkowski and Waskowska 2010)

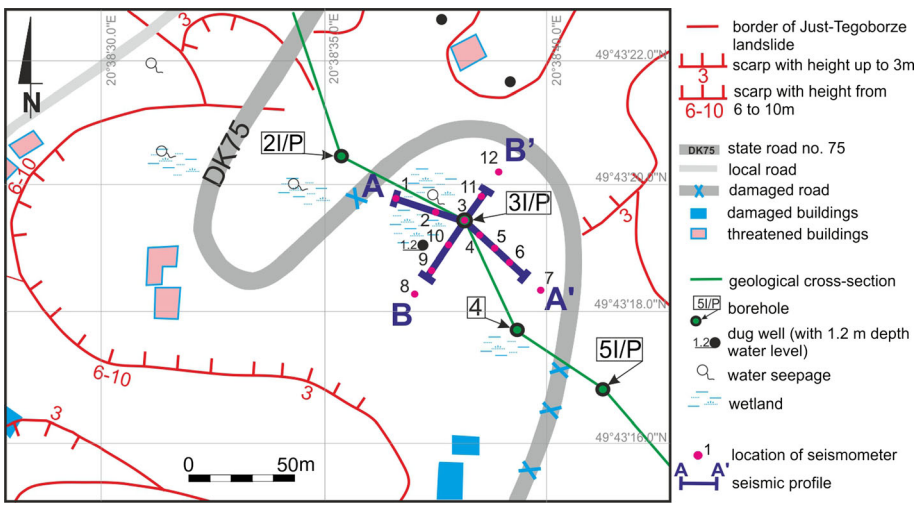

Fig. 3 A part of the Just-Tegoborze landslide sketch on a base topographic map, including projection of a geological engineering cross-section with boreholes and seismic profiles (based on Chowaniec and Wojcik 2012)

Quaternary colluvial deposits cover discordant flysch bedrock on the study area. Strongly cohesive clayey colluvium has a thickness of 10 to 12 m (Fig. 4). It is very heterogenous and consists of clay, humic clay, silty clay, sandy clay, silts, clayey debris, clasts of sandstones, mudstones and shales. Soft clayey colluvium with relocated fragments of soft shales, locally interbedded with hard shales, mudstones and sandstones forms a layer of 3 to 5 m thickness below the near-surface clayey colluvium (Czudec 2012, unpublished data).

Several failure surfaces of the landslide were distinguished as a result of archival geological works (Chowaniec and Wojcik 2012). Failure surfaces were investigated on the study area within colluvial deposits at approximately 10 and 12 m depth and between colluvial deposits and the flysch bedrock at approximately 14 to 17 m depth (Fig. 4).

The Just-Tegoborze landslide developed on the contact between shale and shale-sandstone complexes of Sub-Magura and hieroglyphic beds, and Magura sandstones. Shale and shale-sandstone complexes are less resistant and more susceptible to weathering than Magura sandstones. Magura sandstones have uniaxial compressive strength (UCS) from 19 to 91 MPa, whereas shales from hieroglyphic beds have UCS from 0.25 to 2.9 MPa (Czudec 2012, unpublished data). Other factors, which have an influence on the development of the Just-Tegoborze landslide, include the occurrence of weak variegated shales prone to swelling and complicated tectonics between Magura, Sub-Magura and hieroglyphic beds.

The Just-Tegoborze landslide has southeastern exposure and descends to the Roznow Lake (Fig. 1). The azimuth of its movement is 130°, and its average slope angle is 11.8° (Chowaniec and Wojcik 2012). From a geomorphological point of view, it consists of a number of mass movement areas, however, with no clear boundaries between them. Its slopes are of convex-concave type, and the terrain relief is strongly diversified. Slopes are mostly cut by small coomb valleys, dells and gullies. There are numerous scarps and landslide niches on the upper part of the landslide. On the study area, levels of water filtration were examined on 0.7, 2.0, 4.7 and 5.8 m. Water seepages are observed on the terrain surface close to the 3I/P (Fig. 3). Water level in a dug well, which is located on the study area, is 1.2 m deep, however, it reaches terrain surface during intense rainfalls and spring thaw. It leads to the conclusion that there are weakly permeable deposits which limit the infiltration of water deep into the geological medium. The analysis of the core from 3I/P borehole indicates the presence of low permeable, weakly and medium fractured shales and variegated shales at the depth of 13 m. Above them, there are very fractured shales and previously described colluvial deposits which have a water content up to 35% (Czudec 2012, unpublished data).

Methodology

Seismic acquisition

A local high-frequency seismic noise was used in the study with seismic interferometry, generated mainly by intense vehicle traffic on a state road no. 75 present in the immediate vicinity. Data acquisition was carried out by 12 Güralp CMG-6TD broadband seismometers working autonomously. They were installed along two profiles with lengths of 75 and 95 m, which crossed at the 3I/P borehole (Fig. 3). Distances between seismometers were from 10 to 20 m. Data recording lasted for 60 min with 10 ms sampling. Signals were recorded in the frequency band of 0.03–100 Hz. Figure 5a shows an example of a seismogram of the seismic noise recorded, which is characterized by the strongest seismic energy within a frequency band between 5 and 22 Hz (Fig. 5b). A similar frequency band of vehicle traffic, used as a source for near-surface passive imaging, was studied by Kuzma et al. (2009).

Measurements were carried out in three series in 2015: January 23rd (a dry period), March 9th (a period of an increased water content after the spring thaw) and July 9th (a period of an intense water infiltration during heavy rainfalls). Figure 6 shows a daily average precipitation and temperature measured at nearby

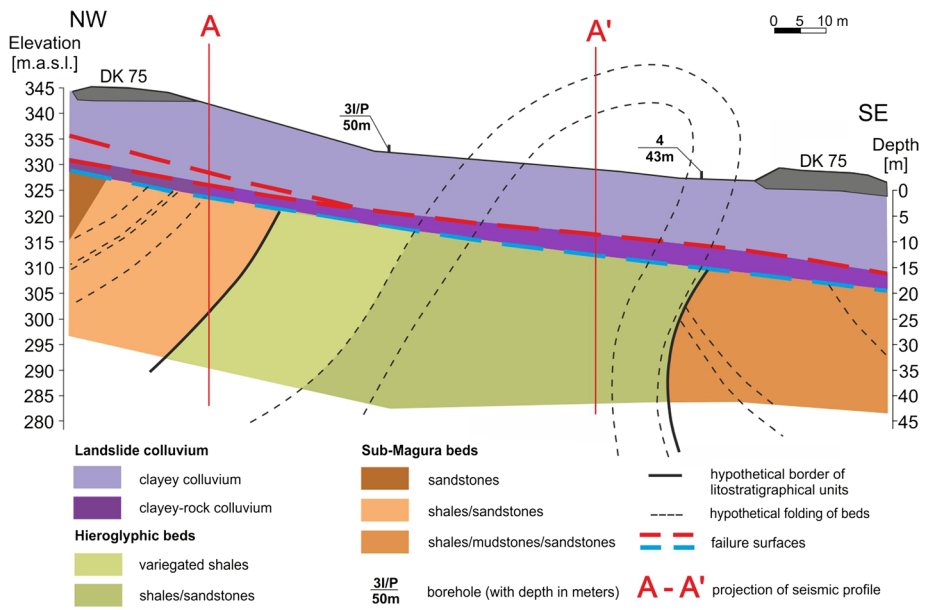

Fig. 4 A part of the geological engineering cross-section of the study area with the A-A′ projected seismic profile (based on Pilecki and Harba 2015)

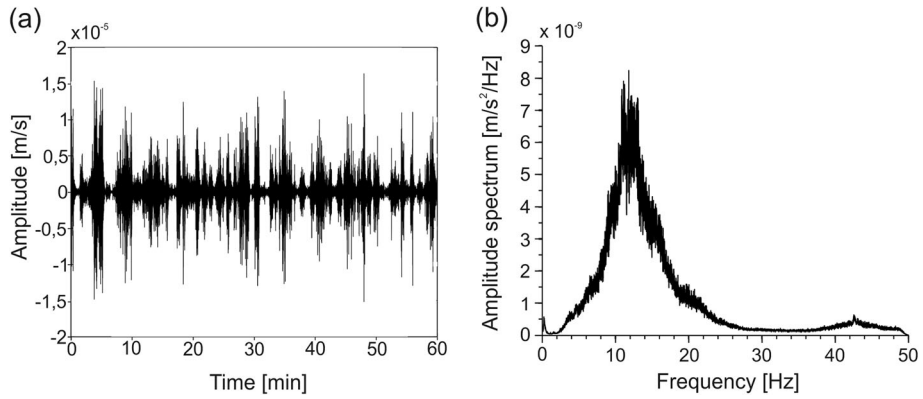

Fig. 5 An example of a seismogram (**a**) and an amplitude spectrum (**b**) of seismic noise recorded in a period of 60 min at the Just-Tegoborze landslide

meteorological stations from July 2014 to July 2015. In each seismic measurement series, the seismometers were installed at the same place. The recognition depth range of the geological medium was up to 20 m.

Processing and interpretation

The data processing and interpretation scheme was similar to those of Bensen et al. (2007) and Cheng et al. (2015).

The measured amplitude records of vertical velocity of ground vibrations on the Just-Tegoborze landslide were first band-pass filtered in the 7 to 35 Hz frequency band for smoothing amplitude spectra. Next, 1-bit normalization and cross-correlation were applied. Cross-correlation functions were computed between all available receiver pairs. As a result, series of empirical Green's functions were obtained and sorted afterwards into the so-called common virtual source gathers for every receiver. Each virtual source was considered as a bidirectional shot with two common virtual source gathers as the causal and acausal signal parts (Fig. 7).

The frequency–wavenumber (f–k) transform was subsequently computed to separate surface wave energy from those of body waves. Muting was applied (Fig. 8a) in order to improve the signal to noise ratio. Finally, the dispersion curve of the Rayleigh wave was extracted (Fig. 8b).

Data interpretation was based on the first picking fundamental modes of the Rayleigh wave from the dispersion curves. They were inverted afterwards to obtain 1D shear wave velocity models (Fig. 9). Inversion was conducted by means of a genetic algorithm. Finally, a 2D shear wave velocity section was constructed on the basis of the 1D information. Data processing and interpretation were carried out using own algorithms written in Matlab and supported by Geogiga Seismic Pro software.

Results and analysis

The seismic sections developed for the three measurement series are presented in Fig. 10 for longitudinal sections and in Fig. 11 for section transverse to the landslide axis.

The 1st measurement series was carried out in the winter period in conditions which may be assumed to be dry (Fig. 6). Evident in this section are three layers with varied S-wave velocities (Fig. 10a). In the near-surface layer, with the lowest

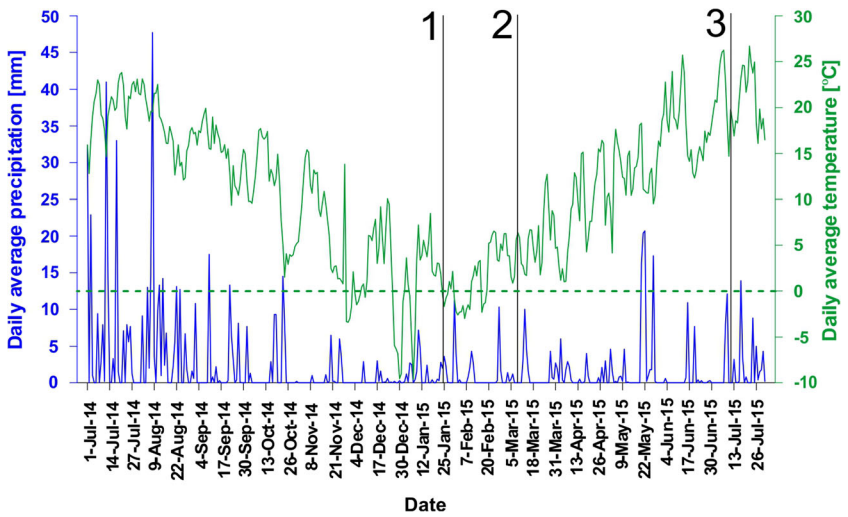

Fig. 6 Daily average precipitation and daily average temperature data measured at the two meteorological stations in the vicinity of the Just-Tegoborze landslide from 1st July 2014 to 31st July 2015. Black vertical lines correspond to measurement series: 1, 2 and 3 respectively

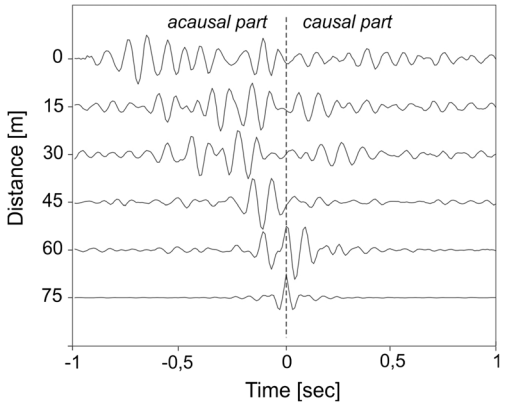

Fig. 7 An example of a common virtual shot gather of the virtual source located at the 75 m point of the B-B′ seismic profile with acausal and causal parts indicated

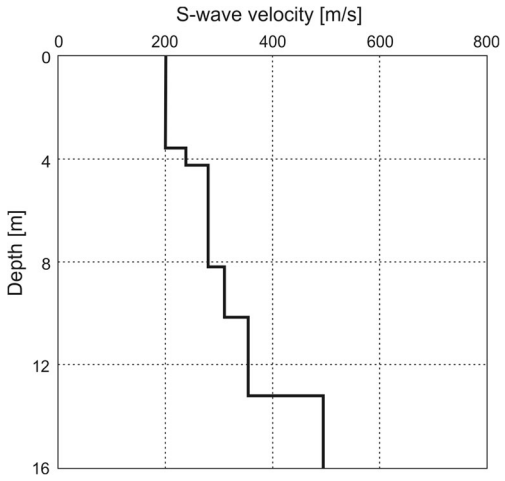

Fig. 9 An example of a 1D S-wave velocity profile inverted from the dispersion curve

velocities ranging from 220 to 270 m/s, there is also a local minimum value in the central part. This layer is most likely connected with the increased water content in the medium, as demonstrated by the observed water table when executing borehole 3I/P and the visible dampness of the terrain surface while taking the measurements. The first layer is characterized by a thickness amounting to approximately 5 m along the entire length of the profile. The next, middle layer is characterized by the S-wave velocity ranging from 270 to 340 m/s. Its thickness is variable and primarily is approximately 8 to 10 m, locally decreasing to 5 m in the 70 to 75 m of the seismic profile (Fig. 10a). Thickness of the second layer is the largest in the central part of the profile. The deepest-located layer is characterized by the S-wave velocity values in the range of 340 to 400 m/s. The roof of this layer occurs at the depth of 10 to 15 m.

The trough-like shape of the seismic boundary between the second and third layers occurs in the zone of the weaker rock mass of the hieroglyphic beds made of clayey variegated shales and shales with instances of minor sandstone interbedding. A harder sandstone-shale rock mass of Sub-Magura beds lies in the vicinity (Fig. 4). The roof of the third layer likely constitutes the surface of a less weathered bedrock.

The 2nd measurement series was carried out in the spring period with a melting snow cover. The near-surface ground might have not yet been fully thawed (Fig. 6). The longitudinal (Fig. 10b) and transverse (Fig. 11a) sections are characterized by a significant decrease in the S-wave velocity in the two surface layers of the medium. In order to emphasize the differences, layer boundaries were marked in the longitudinal section according to contour lines interpreted in Fig. 10a. The zone of weakened elastic properties stretched toward the drop in the terrain surface of the area. The velocity value of the seismic boundary of the bedrock was very slightly changed. It should be noted that the depth of this boundary was maintained.

The 3rd measurement series was conducted in the summer period directly after storm rainfalls (Fig. 6, Fig. 10c, Fig. 11b). Increased infiltration into the medium caused a greater weakening of elastic properties, especially in the first layer, compared to the 2nd series. The velocity value of the seismic boundary of the bedrock again only slightly changed. The depth of this boundary was also maintained. A similar effect may be observed in the transverse sections (Fig. 11a, b).

In relation to the geological engineering cross-section of the research area (Fig. 4), one may notice that the first two near-surface seismic layers correspond to clayey colluvium formations. The seismic

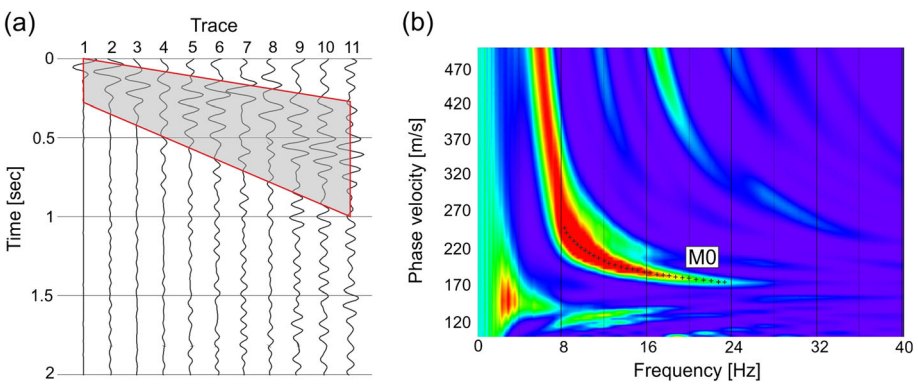

Fig. 8 An example of a seismic noise cross-correlogram with a muting window (**a**) and a dispersion image with a picked fundamental mode (*Mo*) (**b**)

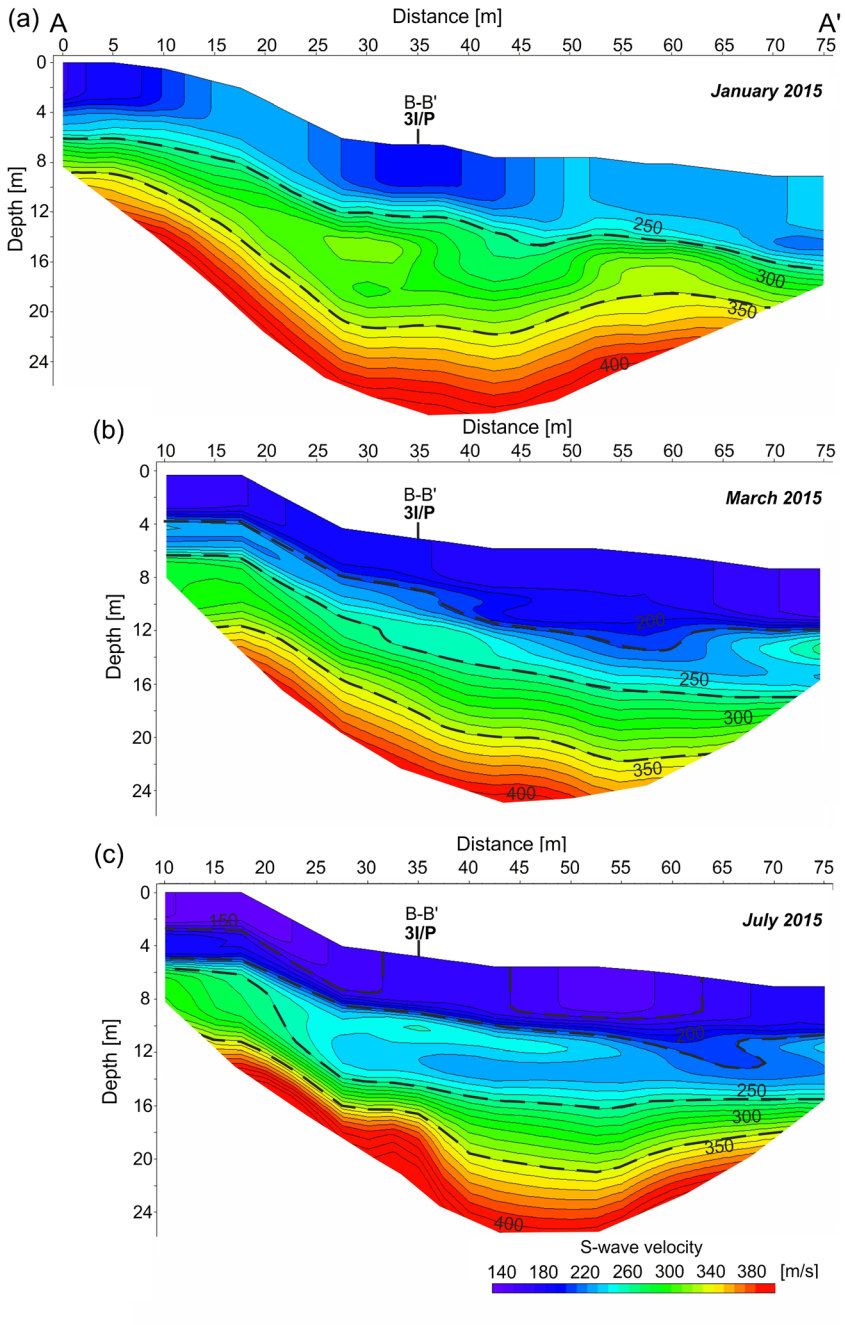

Fig. 10 S-wave velocity section along the A-A′ seismic profile measured on 23rd January 2015 (**a**), 9th March 2015 (**b**) and 9th July 2015 (**c**)

boundary occurring at a depth of approximately 10 to 15 m may be correlated to the roof of the less weathered rock mass of the shale and shale/sandstone series. In the seismic image, the bedrock (third layer) did not undergo significant changes as a result of infiltration, which confirms lesser disturbance by landslide processes in comparison with colluvium layers. Presumably, the bedrock roof boundary is one of the most important failure surfaces of the landslide. The trough-like shape of this seismic boundary in the central part of the seismic section may be connected with the greater range of weathering in the zone of weaker hieroglyphic beds.

Conclusions

This study has demonstrated that it is possible to monitor the changes of shear wave velocities of a geological compound medium, as it is monitored in the Just-Tegoborze landslide by the seismic interferometry method using a local high-frequency ambient noise. The results clearly show changes of the S-wave velocity which are most likely caused by various conditions of infiltration and water content in the geological medium. Generally, an increasing water content in the medium results in the decrease of the S-wave velocity value and also the medium's rigidity.

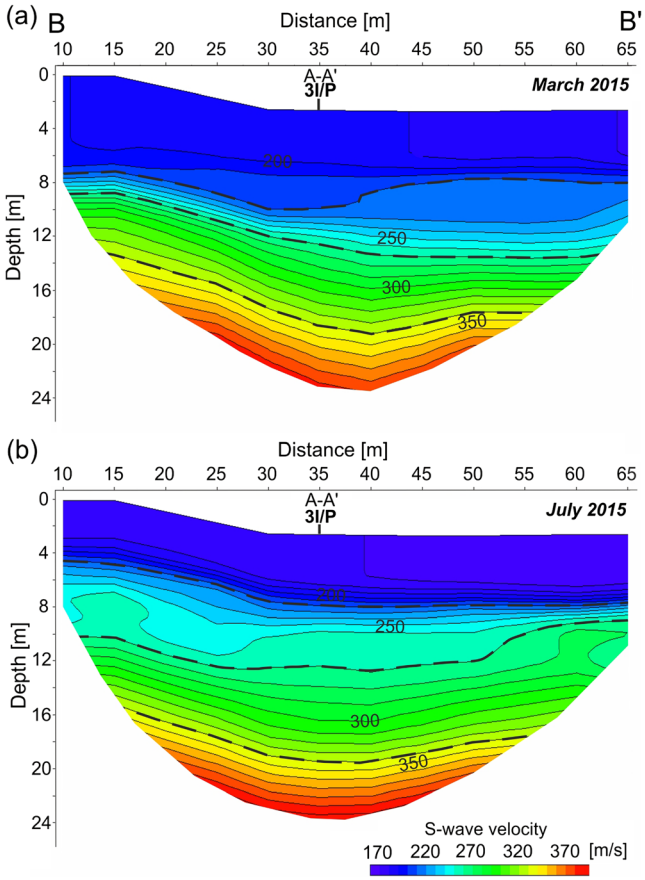

Fig. 11 S-wave velocity section along the B-B′ seismic profile measured on 9th March 2015 (**a**) and 9th July 2015 (**b**)

The interpreted seismic boundaries may be correlated to lithological boundaries shown in a geological engineering cross-section. In the seismic image, the course of the bedrock boundary is more complex in comparison with the geological engineering cross-section. The trough-like shape of this seismic boundary in the central part of the seismic section may be related to the decrease of rigidity of weak hieroglyphic beds compared to the stronger surrounding rock mass, however, it requires further detailed studies. The investigated bedrock boundary is presumably one of the failure surfaces.

The complicated course of the bedrock boundary may also have an influence on the water flow paths in the colluvium layer affected by mass movements. In consequence, it has an influence on the stability of the state road structure.

The presented results of seismic interferometry may be helpful in evaluating the behaviour of the Just-Tegoborze landslide. These findings can be also used in designing protections against mass movements.

Acknowledgements

The article was prepared as a result of the LOFRES project No. PBS1/A2/13/2013 performed within the 1st call of the Applied Research Programme co-financed by the Polish National Centre for Research and Development. We thank the editor and anonymous reviewers for valuable comments and discussions.

References

Aleotti P, Chowdhury R (1999) Landslide hazard assessment: summary review and new perspectives. Bull Eng Geol Environ 58:21–44

Anbarasu K, Sengupta A, Gupta S, Sharma SP (2010) Mechanism of activation of the Lanta Khola landslide in Sikkim Himalayas. Landslides 7:135–147

Barla G, Antolini F, Barla M (2013) Slope stabilization in difficult conditions: the case study of a debris slide in NW Italian Alps. Landslides 10:343–355

Bensen GD, Ritzwoller MH, Barmin MP, Levshin AL, Lin F, Moschetti MP, Shapiro NM, Yang Y (2007) Processing seismic ambient noise data to obtain reliable broad-band surface wave dispersion measurements. Geophys J Int 169:1239–1260

Bichler A, Bobrowsky P, Best M, Douma M, Hunter J, Calvert T, Burns R (2004) Three-dimensional mapping of a landslide using a multi-geophysical approach: the Quesnel Forks landslide. Landslides 1:29–40

Bièvre G, Jongmans D, Goutaland D, Pathier E, Zumbo V (2015) Geophysical characterization of the lithological control on the kinematic pattern in a large clayey landslide (Avignonet, French Alps). Landslides. doi:10.1007/s10346-015-0579-0

Bogoslovsky VA, Ogilvy AA (1977) Geophysical methods for the investigation of landslides. Geophysics 42(3):562–571

Bonnard C, Corominas J (2005) Landslide hazard management practices in the world. Landslides 2:245–246

Brückl E, Brunner FK, Lang E, Mertl S, Müller M, Stary U (2013) The Gradenbach Observatory—monitoring deep-seated gravitational slope deformation by geodetic, hydrological, and seismological methods. Landslides 10:815–829

Cascini L, Bonnard C, Corominas J, Jibson R, Montero-Olarte J (2005) Landslide hazard and risk zoning for urban planning and development. In: Hungr O, Fell R, Couture R, Eberhardt E (eds) Landslide risk management, proceeding of the international conference on landslide risk management, Vancouver, Canada. A.A. Balkema Publishers, Taylor & Francis Group, London, pp. 199–235

Cheng F, Xia J, Xu Y, Xu Z, Pan Y (2015) A new passive seismic method based on seismic interferometry and multichannel analysis of surface waves. J Appl Geophys 117:126–135

Chowaniec J, Wojcik A (eds) (2012) Landslides in Malopolskie voivodeship, A guidebook (in Polish). Carthographic Publishing House Compass, Krakow, pp. 89–91

Cieszkowski M, Waskowska A (2010) Castles from the Roznow and Czchow lakes area as geotouristic lapidarium and role of the Istebna Sandstones in their construction (in polish). Geotourism 2(21):3–18

Curtis A, Gerstoft P, Sato H, Snieder R, Wapenaar K (2006) Seismic interferometry – turning noise into signal. Lead Edge 25:1082–1092

Czudec G (2012) Geological-engineering documentation for developing landslide stabilization no. MPL0051, on the state road no. 75, 51 + 900 do 52 + 700 km in Tegoborze-Just, Lososina Dolna commune, Nowy Sacz county, Malopolskie voivodeship. Geotech Sp. z o.o. Archive no. 1266 (in Polish) – unpublished data

Dai FC, Lee CF, Ngai YY (2002) Landslide risk assessment and management: an overview. Eng Geol 64:65–87

Del Gaudio V, Wasowski J, Muscillo S (2013) New developments in ambient noise analysis to characterise the seismic response of landslide-prone slopes. Nat Hazards Earth Syst Sci 13:2075–2087

Guzzetti F, Carrara A, Cardinali M, Reichenbach P (1999) Landslide hazard evaluation: a review of current techniques and their application in a multi-scale study, Central Italy. Geomorphology, vol 31:181–216

Frasheri A, Kapllani L, Dhima F (1998) Geophysical landslide investigation and prediction in the hydrotechnical works. Journal of the Balkan Geophysical Society 1(3):38–43

Fukuoka H, Sassa K, Wang G, Wang F, Wang Y, Tian Y (2005) Landslide risk assessment and disaster management in the Imperial Resort Palace of Lishan, Xian, China. In: Sassa K, Fukuoka H, Wang G, Wang F (eds) Landslides, Risk Analysis and Sustainable Disaster Management. Springer, Berlin Heidelberg, pp. 81–89

Hack R (2000) Geophysics for slope stability. Surv Geophys 21:423–448

Hibert C, Grandjean G, Bitri A, Travelletti J, Malet J-P (2011) Characterizing landslides through geophysical data fusion: example of the La Valette landslide (France). Eng Geol 128:23–29
Jongmans D, Bièvre G, Renalier F, Schwartz S, Beaurez N, Orengo Y (2009) Geophysical investigation of a large landslide in glaciolacustrine clays in the Trièves area (French Alps). Eng Geol 109:45–56
Jongmans D, Garambois S (2007) Geophysical investigation of landslides: a review. Bulletin de la Société Géologique de France 178(2):101–112
Kuzma HA, Fernández-Martínez JL, Zhao Y, Dunson C, Zhai M, Mangriotis M, Rector JW (2009) Vehicle traffic as a source for near-surface passive seismic imaging. Symposium on the Application of Geophysics to Engineering and Environmental Problems 2009:609–615
Larose E, Carrière S, Voisin C, Bottelin P, Baillet L, Guéguen P, Walter F, Jongmans D, Guiller B, Garambois S, Gimbert F, Massey C (2015) Environmental seismology: what can we learn on Earth processes with ambient noise? J Appl Geophys 116:62–74
Lundström K, Larsson R, Dahlin T (2009) Mapping of quick clay formations using geotechnical and geophysical methods. Landslides 6:1–15
Mainsant G, Chambon G, Jongmans D, Larose E, Baillet L (2015) Shear-wave-velocity drop prior to clayey mass movement in laboratory flume experiments. Eng Geol 192:26–32
Mainsant G, Jongmans D, Chambon G, Larose E, Baillet L (2012a) Shear-wave velocity as an indicator for rheological changes in clay materials: lessons from laboratory experiments. Geophys Res Lett 39:L19301
Mainsant G, Larose E, Brönnimann C, Jongmans D, Michoud C, Jaboyedoff M (2012b) Ambient seismic noise monitoring of a clay landslide: toward failure prediction. J Geophys Res 117:F01030
Mansour MF, Morgenstern NR, Martin CD (2011) Expected damage from displacement of slow-moving slides. Landslides 8:117–131
Méric O, Garambois S, Jongmans D, Wathelet M, Chatelain JL, Vengeon JM (2005) Application of geophysical methods for the investigation of the large gravitational mass movement of Séchilienne, France. Can Geotech J 42:1105–1115
Méric O, Garambois S, Malet J-P, Cadet H, Gueguen P, Jongmans D (2007) Seismic noise-based methods for soft-rock landslide characterization. Bulletin de la Société Géologique de France 178(2):137–148
Pilecki Z, Harba P (2015) Structure and properties of a landslide investigated with seismic interferometry using high-frequency seismic noise—preliminary results (in polish). Bulletin of the Mineral and Energy Economy Research Institute of the Polish Academy of Sciences 89:63–76
Pilz M, Parolai S, Bindi D, Saponaro A, Abdybachaev U (2013) Combining seismic noise techniques for landslide characterization. Pure Appl Geophys 171(8):1729–1745
Renalier F, Bièvre G, Jongmans D, Campillo M, Bard P-Y (2010a) Clayey landslide investigations using active and passive V_s measurements. In: Miller RD, Bradford JH, Holliger K (eds) Advances in near-surface seismology and ground-penetrating radar, Geophys. dev. Ser, vol 15. Society of Exploration Geophysicists, Tulsaa, pp. 397–414
Renalier F, Jongmans D, Campillo M, Bard P-Y (2010b) Shear wave velocity imaging of the Avignonet landslide (France) using ambient noise cross correlation. J Geophys Res 115:F03032
Reynolds JM (2011) An introduction to applied and environmental geophysics, 2nd edn. Wiley-Blackwell Publishing, Chichester
Salas-Romero S, Malehmir A, Snowball I, Lougheed BC, Hellqvist M (2015) Identifying landslide preconditions in Swedish quick clays – insights from integration of surface geophysical, core sample- and downhole property measurements, DOI:10.1007/s10346-015-0633-y
Sassa K, Wang G, Fukuoka H, Wang F, Ochiai T, Sugiyama M, Sekiguchi T (2004) Landslide risk evaluation and hazard zoning for rapid and long-travel landslides in urban development areas. Landslides 1:221–235
Schuster GT (2009) Seismic interferometry. Cambridge University Press, New York
Singh RP, Dubey CS, Singh SK, Shukla DP, Mishra BK, Tajbakhsh M, Ningthoujam PS, Sharma M, Singh N (2013) A new slope mass rating in mountainous terrain, Jammu and Kashmir Himalayas: application of geophysical technique in slope stability studies. Landslides 10:255–265
Song Y-S, Kim K-S (2014) Geotechnical properties of landslide sites in Korea with differing geology. In: Sassa K, Canuti P, Yin Y (eds) Landslide science for a safer Geoenvironment, Volume 2: Methods of Landslide Studies. Springer International Publishing Switzerland, Cham, pp. 87–92
Travelleti J, Malet J-P, Samyn K, Grandjean G, Jaboyedoff M (2013) Control of landslide retrogression by discontinuities: evidence by the integration of airborne- and ground-based geophysical information. Landslides 10:10–54
Wapenaar K, Draganov D, Snieder R, Campman X, Verdel A (2010a) Tutorial on seismic interferometry: part 1—basic principles and applications. Geophysics 75(5):75A195–75A209
Wapenaar K, Slob E, Snieder R, Curtis A (2010b) Tutorial on seismic interferometry: part 2—underlying theory and new advances. Geophysics 75(5):75A211–75A227
Xia J, Miller RD, Park CB (1999) Estimation of near-surface shear-wave velocity by inversion of Rayleigh waves. Geophysics 64(3):691–700
Zarroca M, Linares R, Roqué C, Rosell J, Gutiérrez F (2014) Integrated geophysical and morphostratigraphic approach to investigate a coseismic (?) translational slide responsible for the destruction of the Montclus village (Spanish Pyrenees). Landslides 11:655–671

P. Harba (✉) · Z. Pilecki
The Mineral and Energy Economy Research Institute of the Polish Academy of Sciences, Wybickiego 7, 31-261, Krakow, Poland
e-mail: paulina@meeri.eu